

Forward Raman Instability and Electron Acceleration

C. Joshi, T. Tajima,^(a) and J. M. Dawson

Center for Plasma Physics and Fusion Engineering, University of California, Los Angeles, California 90024

and

H. A. Baldis

Division of Physics, National Research Council of Canada, Ottawa K1A 0R6, Canada

and

N. A. Ebrahim

Department of Engineering and Applied Science, Yale University, New Haven, Connecticut 06520

(Received 30 March 1981)

It is demonstrated by experiments and supporting particle simulations that the forward Raman instability is capable of producing extremely high-energy electrons in an underdense plasma. The instability has a high saturation level for the electrostatic wave component. Its consequences and applications to the laser electron accelerator and the laser-fusion pellet preheat are discussed.

PACS numbers: 42.65.Cq, 52.35.Mw, 52.25.Ps, 52.60.+h

Although Raman backscatter has been under active investigation lately,¹ the Raman forward scattering (RFS) instability has hitherto received relatively little attention.² We demonstrate, however, in this Letter that RFS can dominate backscatter when the pump is reasonably strong and/or the electron temperature is high for underdense plasmas. Furthermore, extremely relativistic electrons are produced by the nonlinear damping of the high-phase-velocity electron plasma waves (EPW) characteristic of the RFS process. In this Letter we present results from an experiment which looks directly at forward-emitted electrons from a high-temperature, underdense plasma irradiated by an intense CO₂-laser pulse. Relativistic electromagnetic particle simulations of the experiment indeed confirm that RFS is responsible for the observed electron acceleration to relativistic energies.

The role of RFS in ultrahigh-energy electron generation was investigated experimentally and checked against particle simulations by using the same relevant parameters. 130-Å-thick, self-supported carbon foils were irradiated at normal incidence by intense, $v_0/c \sim 0.3$, 700-ps full width at half maximum, CO₂-laser pulses. $v_0 = eE_0/m\omega_0$ is the quivering velocity in the laser field. 1%-5% of the incident energy was backscattered and roughly 50% of the incident energy was transmitted by the plasma. Thus it can be assumed that the foil plasma becomes underdense around the peak of the laser pulse. The electron temperature of the bulk distribution was deduced from the slope of the ion spectra, recorded absolutely

by use of Thomson parabolas, to be ~ 20 keV for both front and rear expansions. The angular distribution of the electrons escaping the plasma was measured with two absolutely calibrated electron spectrometers in the range 0.4–1.5 MeV.

Figure 1 shows the absolute electron spectra measured at $\theta \approx 5^\circ$ in the forward direction and $\theta \approx 15^\circ$ in the backward direction from the thin

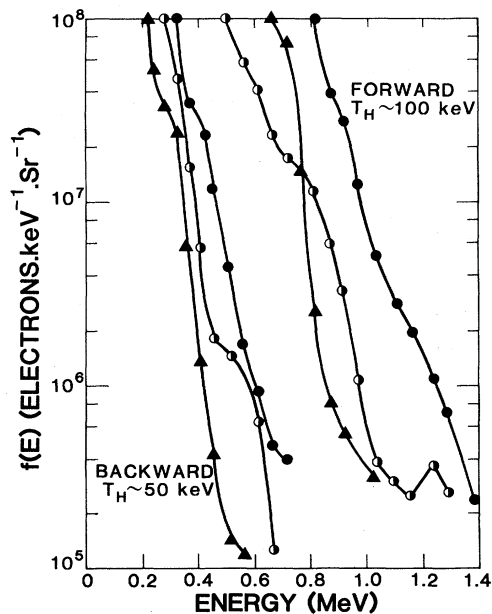


FIG. 1. Experimental electron energy distributions in the forward and backward directions. Three different shots are represented.

carbon foil plasmas. If a Maxwellian distribution is assumed then these distributions can be characterized by temperatures of 90–100 keV in the forward direction and of 40–50 keV in the backward direction. Electrons with energies up to 1.4 MeV were observed in the forward direction. The highest energy electron emission (>1 MeV) was strongly peaked in the direction of the laser. Electrons up to 400 keV were observed nearly isotropically, however, probably attributable to $2\omega_p$ decay and Raman sidescattering. By integration over the measured angular distribution, assuming azimuthal symmetry, $\sim 10^{11}$ electrons with energy greater than 400 keV are found to escape the plasma. Although no direct measurements of the target potential due to this loss of electrons were made, we note that target potentials of ~ 200 keV have been measured under similar irradiance conditions.³

A simple estimate shows that RFS is important in our experiment. The growth rate for the RFS process⁴ is given by $\gamma = \frac{1}{2}(v_0/c)\omega_p^2/\omega_0$ and the finite-length limit on growth is $\gamma L/(cv_g)^{1/2} > 1$, where $v_g = 3k_p v_e^2/\omega_p$ and L is the interaction length. Assuming $v_0/c \sim 0.3$, $T_e \sim 20$ keV, and $\omega_p/\omega_0 \sim 0.46$, we obtain for $L/\lambda \sim 50$, $\gamma/\omega_0 \sim 0.03$, and we have nearly 27 e -folding growths from the initial noise level. If instead of the resonant three-wave process we assume induced scattering by the resonant electrons (stimulated Thomson scattering) then the growth rate is smaller by a factor v_0/c . For backscatter the growth rates are comparable to those for the forward scatter but backscatter suffers much more severe Landau damping due to the shorter wavelength and the lower phase velocity of the backward EPW. The assumption of a homogeneous plasma with $L/\lambda \sim 50$ is reasonable, since we expect the instability to occur in the density plateau region, separating the front and the rear expansions. This region has a density scale length somewhere in between the focal spot diameter (150 μm) and the ion acoustic speed times the pulse-length full width at half maximum (1000 μm). In any case the depth of focus of the laser beam was ~ 50 wavelengths.

Simulations were carried out on the one-dimensional relativistic electromagnetic particle code⁵ with the periodic boundary conditions where similar wave setups were used as before.⁶ The plasma was initially thermal, $T_e \sim 20$ keV, and uniform, $\omega_p/\omega_0 \sim 0.46$. The propagating electromagnetic pulse has $v_0/c \sim 0.3$. The distribution function $f(p_{\parallel})$ as well as the electrostatic wave spec-

tra are displayed in Fig. 2. The temperature and the maximum electron energy observed in the simulation distributions were similar to the experimentally measured values. For instance, simulations show electrons with $(\epsilon_{\text{max}})_F \approx 1.3$ MeV and $(T_{\text{hot}})_F \sim 100$ keV in the forward direction compared to experimental values $(\epsilon_{\text{max}})_F \sim 1.4$ MeV and $(T_{\text{hot}})_F \sim 90$ –100 keV. Similarly, simulations show $(\epsilon_{\text{max}})_B \sim 0.9$ MeV and $(T_{\text{hot}})_B \sim 60$ keV in the backward direction compared to experimental values of $(\epsilon_{\text{max}})_B \sim 0.8$ MeV and $(T_{\text{hot}})_B \sim 40$ –50 keV. In view of the possible influence of the target potential on the experimentally measured electron distributions, this rather excellent agreement between the experiment and the simulations may be rather fortuitous, particularly for the maximum electron energy, unless the target potential was indeed much smaller than ϵ_{max} . The electrostatic wave spectrum [Fig. 2(b)] shows that the backscatter mode k_b (which grows initially) is swamped by other modes with a smaller wave number, the most intense of which is the plasma wave associated with forward scatter, k_p . In addition, there are some wave numbers which are less than k_p .⁷ Thus the heated electron

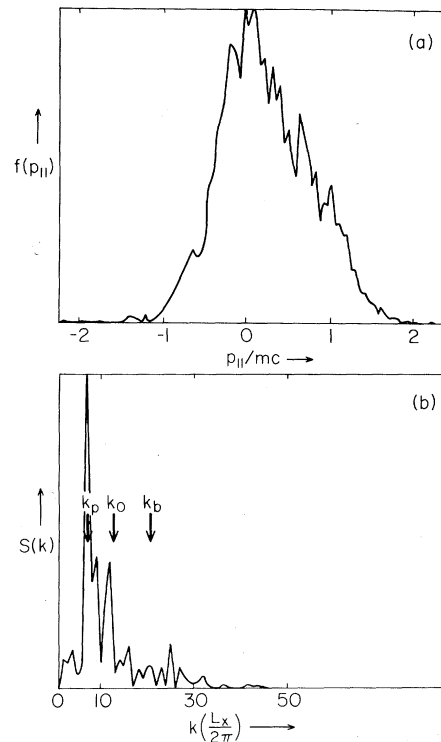


FIG. 2. Simulation (under the same conditions as in Fig. 1) of electron energies (a) at $t = 250\omega_p^{-1}$ as well as (b) the electrostatic mode spectra at $t = 100\omega_p^{-1}$.

distributions obtained by the experiment and the simulations agree well with most of the electron heating due to the RFS process (and/or multiple RFS⁸ processes since repeated k matching is possible only for the RFS process), but is not so much due to the backward process.

The reason why the backscattering is suppressed is the following: When the backscattering EPW is excited, heavy Landau damping or electron trapping by this EPW saturates it at a low level thus limiting the backscattering to a small value. The phase velocity of the backscattering EPW is $v_p = \omega_p/k_b$ which for this case is $\sim 1.6v_e$. Thus this wave is heavily Landau damped to begin with and as it grows in amplitude, more and more particles will be trapped by it and the damping will grow. The trapping width⁹ is given approximately by $\Delta v_t = (2eE_{EPW}v_p/m\omega_p)^{1/2}$, where E_{EPW} is the electric field for the plasma wave. The condition that a large number of electrons are trapped is given¹⁰ by $v_p - \Delta v_t \lesssim 2v_e = 2(T_e/m)^{1/2}$. The maximum electrostatic wave intensity is obtained for a cold plasma by setting $v_e = 0$. This gives for the saturation amplitude E_{EPW} for the longitudinal wave as $(eE_{EPW}/m\omega_p) = v_p/2$. For our case, the phase velocity is $O(v_e)$ and we expect little growth; in any case, the saturation in-

tensity for a cold plasma is less than 6% of the light waves. In addition the two-plasmon-decay instability would also saturate at a low level even if ω_0 were chosen to be $2\omega_p$ because strong Landau damping sets in much earlier for $2\omega_p$ decay than it does for the forward Raman process. The RFS process appears to be the last parametric process to saturate in this hot underdense plasma. In fact it can be argued that it will saturate only when the original electromagnetic wave has completely cascaded by multiple RFS to waves near $\omega_0 \simeq \omega_p$.

Quite clearly, relativistic-energy electron production by RFS is a phenomenon of possibly great importance to a number of fields: laser fusion, laser electron accelerator,⁶ cascade plasma heating of solenoid plasmas,⁸ traveling-wave pump for x-ray lasers, and trident-pair production in laser plasmas, to name a few. For very intense laser irradiation of a large underdense plasma of a laser-fusion pellet, relativistic electrons produced by RFS may penetrate and preheat any reasonable amount of shielding around the D-T fuel. However, in most applications (e.g., the laser electron accelerator) a narrow-divergence, small-energy-spread electron beam is desired. This can be achieved by injecting two parallel laser beams ω_0, k_0 and ω_1, k_1 in the underdense plasma with the condition $\omega_p = \omega_0 - \omega_1$. In this case, optical mixing¹¹ can generate an EPW at $k_p = k_0 - k_1$ with phase velocity nearly equal to the group velocity of the light waves.

We have also simulated this process using the parameters $\omega_0 = 4.29\omega_p$, $\omega_1 = 3.29\omega_p$, and each beam amplitude $v_i = eE_i/m\omega_i = c$ ($i = 0$ or 1). Figure 3 shows the phase space of electrons accelerated by the beat wave $k_p \simeq \omega_p/c$. High-energy electrons are seen in every ridge of each wave-

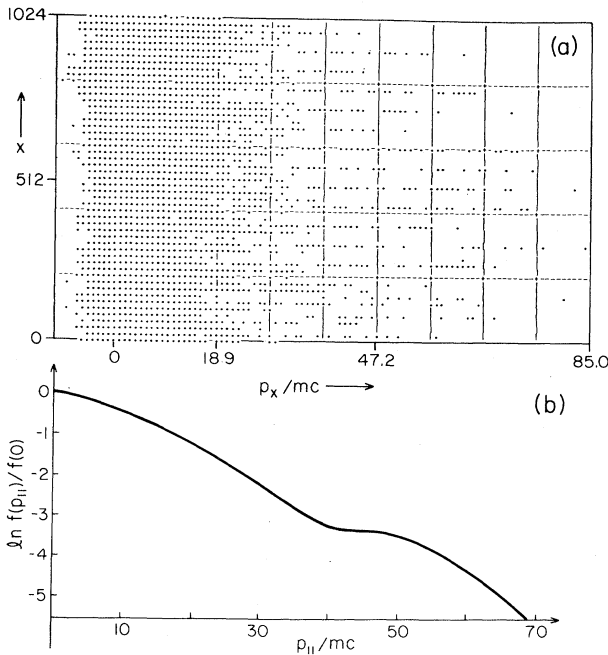


FIG. 3. Photon beat acceleration by two beams (ω_0, k_0) and (ω_1, k_1). (a) The electron phase space (x, p_s) at $t = 240\omega_p^{-1}$. The maximum $\gamma_{||}$ for electrons is 85 in this case. (b) The logarithm of the electron distribution function at $t = 135\omega_p^{-1}$.

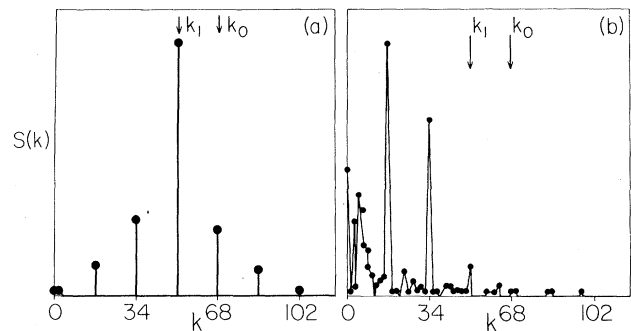


FIG. 4. The electromagnetic energy distribution as a function of mode numbers. Pumps k_0 and k_1 are indicated by arrows. (a) $t = 142.5\omega_p^{-1}$, (b) $t = 240\omega_p^{-1}$.

length of the resonantly excited EPW. In this case the parameters are $v_e = 1\omega_p\Delta$, $c = 10\omega_p\Delta$, the system length 1024Δ , and 10240 particles, with Δ being the grid spacing. The maximum electron energy reached was $85mc^2$, which is a little higher than the theoretical value of $\epsilon_{\text{max}} \sim 2mc^2(\omega_0/\omega_p)^2$. One reason for this discrepancy may be that we now have two intense electromagnetic waves so that magnetic acceleration associated with $v_0 \times B_1$ and $v_1 \times B_0$ also begins to play a role.¹² The distribution function $f(v_{\parallel})$ is shown in Fig. 3(b), exhibiting intense main body heating as well as an extremely energetic tail. Figures 4(a) and 4(b) show the electromagnetic energy spectra of the system at two different times. At the earlier time the originally two-peaked structure at k_0 and k_1 already shows a downward cascade, while some small amount of energy is up-converted. The spectrum is sharply peaked at a particular discrete wave number $k_n = k_0 - nk_p$ where n is an integer. The spectral density $S(k, \omega)$ (not displayed here) for the electrostatic component shows no significant energy in any frequency at the backscattered wave numbers $k_b = 1.77k_0$ or $1.3k_0$. This strongly suggests that all possible backscattering processes are suppressed or saturated at a very low level in our present problem. The electrostatic spectral density $S(k, \omega)$ at the resonant plasma wave number $k = k_p$ is very intense with some energy at the multiple harmonics $k = nk_p$. All these observations confirm that the downward photon cascade is due to the multiple forward Raman scattering.

In conclusion, experimental results and computer simulations presented in this Letter demonstrate that RFS is capable of producing extremely relativistic-energy electrons in hot, underdense plasmas. This instability may be an important source of preheat-causing electrons in long-pulse laser-fusion experiments. On the other hand, it makes the two-beam-beat laser electron accelerator attractive.

The work was supported by the U. S. Depart-

ment of Energy under Contracts No. DE-FG05-80 and No. ET 53088, the National Science Foundation under Grants No. PHY-79-01319 and No. 4-442520-21844, and by the Los Alamos Scientific Laboratory under Contract No. 4-XPO-1033P-1. Stimulating discussions with Professor F. F. Chen, C. E. Clayton, Dr. K. Estabrook, and Dr. J. M. Kindel are acknowledged with pleasure.

^(a)Present address: Institute for Fusion Studies, University of Texas at Austin, Austin, Tex. 78712.

¹D. Phillion and D. L. Banner, Lawrence Livermore Laboratory Report No. UCRL-84854 L, 1980 (unpublished); N. A. Ebrahim, C. Joshi, and H. A. Baldis, University of California, Los Angeles, Report No. PPG-525 (to be published); R. G. Watt, R. D. Brooks, and Z. A. Pietrzyk, Phys. Rev. Lett. **41**, 170 (1970).

²K. Estabrook, W. L. Kruer, and B. F. Lasinski, Phys. Rev. Lett. **45**, 1399 (1980).

³R. F. Benjamin, G. H. McCall, and A. W. Ehler, Phys. Rev. Lett. **42**, 890 (1979).

⁴J. J. Thomson, Phys. Fluids **21**, 2082 (1978).

⁵A. T. Lin, J. M. Dawson, and H. Okuda, Phys. Fluids **17**, 1995 (1974).

⁶T. Tajima and J. M. Dawson, Phys. Rev. Lett. **43**, 267 (1979).

⁷These modes would correspond to the "beam modes" generated by the forward accelerated electrons. In the single-pump case of $\omega_0 = 4.3\omega_p$, similar dominance by the forward-scattering process is observed. However, in this case there are no significant electrostatic modes with $k < k_p$.

⁸B. I. Cohen, A. N. Kaufman, and K. M. Watson, Phys. Rev. Lett. **29**, 581 (1972).

⁹The formula is nonrelativistic, but is sufficiently accurate for the present purpose. Also see the footnote in Ref. 6.

¹⁰J. M. Dawson and R. Shanny, Phys. Fluids **11**, 1506 (1968).

¹¹M. N. Rosenbluth and C. S. Liu, Phys. Rev. Lett. **29**, 701 (1972).

¹²M. Ashour-Abdalla, J. N. Leboeuf, T. Tajima, J. M. Dawson, and C. F. Kennel, Phys. Rev. A **23**, 1406 (1981).